

Phase analysis of image states and surface states associated with nearly-free-electron band gaps

N. V. Smith

AT&T Bell Laboratories, Murray Hill, New Jersey 07974

(Received 3 May 1985)

Surface-state occurrence on low-index faces of metals is analyzed with use of a combination of elementary multiple-reflection theory and elementary nearly-free-electron (NFE) theory. Five NFE gaps on Cu are considered in detail, three associated with the bulk L gap at $\bar{\Gamma}$:Cu(111), \bar{Y} :Cu(110), and \bar{X} :Cu(001), and two associated with the bulk X gap at $\bar{\Gamma}$:Cu(001) and \bar{X} :Cu(110). The predicted surface states, of both the image-potential-induced and crystal-induced kinds, are all intimately related through the phases of the multiple-reflection approach, and their energies are in reasonable accord with photoemission and inverse-photoemission measurements. An empirical curve for the energy dependence of the barrier phase change spanning the changeover region between steplike and imagelike behavior is proposed. Effective masses, surface corrugation, and the effects of work-function variation are also discussed.

I. INTRODUCTION

The recent spectroscopic detection of image-potential-induced surface states using inverse photoemission¹⁻⁵ has aroused new interest⁶ in the multiple-reflection theory of surface-state formation.⁷⁻⁹ The attractive feature of this model is that it generates both the image states and the "crystal-induced" surface states, and that the connection between them is displayed as a simple phase relation.

The aim of this paper is to examine the systematics of surface-state occurrence in bulk band gaps on different crystal faces of metals. The procedure is to combine elementary multiple-reflection theory with elementary nearly-free-electron (NFE) theory.¹⁰⁻¹³ These basic ingredients are far from new, but they have not been assembled before in quite this way or for this particular purpose. As examples, we shall consider ten surface states associated with five nearly-free-electron gaps distributed over the three low-index faces of copper: Cu(111), Cu(001), and Cu(110). The paper will include also discussion of effective masses, surface corrugation, and the effects of varying the work function.

II. MULTIPLE-REFLECTION APPROACH

The essence of the multiple-reflection approach is illustrated in the energy diagram of Fig. 1. The crystal potential is taken to terminate at some plane. Beyond this plane the potential will be barrierlike and must have an asymptotic image form. We shall take the z axis along the outward surface normal and the $z=0$ origin at the outermost atomic layer. Adopting the nomenclature of Echenique and Pendry,⁹ we denote by $r_C e^{i\phi_C}$ and $r_B e^{i\phi_B}$ the respective electron reflectivities. Bound surface states occur when

$$\phi \equiv \phi_C + \phi_B = 2\pi n, \quad (1)$$

where n is an integer. This is a Bohr-like quantization condition on the round-trip phase accumulation ϕ .

A. Barrier phase change ϕ_B

For a pure image potential, the barrier phase change may be written^{7,14} as a simple function of the vacuum energy E_V and the perpendicular energy ϵ :

$$\phi_B/\pi = [(3.4 \text{ eV})/(E_V - \epsilon)]^{1/2} - 1, \quad (2)$$

$$\epsilon \equiv E - \hbar^2 k_{\parallel}^2 / 2m \equiv \hbar^2 k^2 / 2m. \quad (3)$$

E is the electron energy measured from the bottom of the inner potential well, and $k_{\parallel} \equiv (k_x^2 + k_y^2)^{1/2}$ is the parallel wave vector. For saturated barriers (i.e., those which join continuously to the crystal potential), ϕ_B is generally obtained by integrating Schrödinger's equation along the z axis.¹⁴ The expression of Eq. (2) will suffice, however, for much of the approximate discussion of this paper. In Sec.

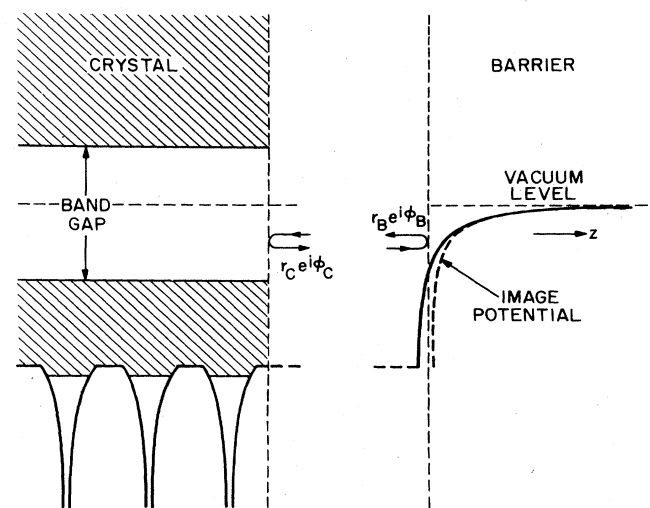


FIG. 1. Schematic potential in the vicinity of a crystal surface. Surface states arise through multiple reflection between the terminating plane of the crystal and the surface barrier.

IV C we shall consider an empirical, and more physical, form for ϕ_B .

The form of ϕ_B for an abrupt step-potential barrier is

$$\tan(\phi_B/2) = -[(E_V - \epsilon)/\epsilon]^{1/2}. \quad (4)$$

Note that on approaching E_V , the phase for a step barrier varies as $(E_V - \epsilon)^{1/2}$, whereas that for an image barrier diverges as $(E_V - \epsilon)^{-1/2}$, permitting Eq. (1) to be satisfied *ad infinitum*, generating a Rydberg series converging on the vacuum level. Herein lies the fundamental physical difference between a short-range step potential and a long-range image potential.

B. Crystal phase change ϕ_C

If ϕ_C can be treated as constant over the range of the Rydberg series, the energies are given by⁷

$$E = E_V - e_n + \hbar^2 k_{||}^2 / 2m, \quad (5)$$

$$e_n = (0.85 \text{ eV}) / (n+a)^2, \quad n = 1, 2, 3, \dots \quad (6)$$

$$a = \frac{1}{2}(1 - \phi_C/\pi). \quad (7)$$

In conformity with hydrogenic terminology, the numbering sequence of the image states is taken to start at $n=1$. For the infinite-crystal-barrier case ($a=0$), the wave function of the $n=1$ state has no node beyond the image plane, the $n=2$ state has one node, and so on.

Over the energy range of a band gap, it becomes necessary to take explicit account of the variation of ϕ_C with E . This topic is the subject matter of Sec. III. In particular, it will be shown that in that case of a Shockley-inverted gap there can exist an additional ($n=0$) surface state lying at an energy below the lowest state ($n=1$) of the image-potential Rydberg series.

III. NEARLY-FREE-ELECTRON BAND GAPS

Electron energies in the NFE two-band model are given by

$$\begin{vmatrix} (\hbar^2/2m)\mathbf{k}^2 - E & V_g \\ V_g & (\hbar^2/2m)(\mathbf{k} - \mathbf{g})^2 - E \end{vmatrix} = 0. \quad (8)$$

On the zone boundary associated with the reciprocal-lattice vector \mathbf{g} , there is a gap of magnitude $2|V_g|$. Within the gap, solutions with real E are still possible, provided we set $k_z = p + iq$, corresponding to wave functions which decay away from the surface into the bulk.¹⁰

A. "One-dimensional" case

The easiest case occurs when \mathbf{g} is along the surface normal. The real and imaginary parts of Eq. (8) immediately yield the standard results

$$p = g_z/2, \quad (9)$$

$$(\hbar^2/2m)q^2 = (4\epsilon E_g + V_g^2)^{1/2} - (\epsilon + E_g), \quad (10)$$

$$E_g = (\hbar^2/2m)(g_z/2)^2, \quad (11)$$

$$\sin(2\delta) = -(\hbar^2/2m)(pq/V_g). \quad (12)$$

The corresponding wave function inside the crystal is

$$\psi = e^{qz} \cos(pz + \delta). \quad (13)$$

We shall be interested primarily in the Shockley-inverted case, where the gap is *p*-like at the bottom and *s*-like at the top. Since we take the origin of coordinates on a surface atom, this case corresponds to $V_g > 0$, and the phase parameter δ varies from $-\pi/2$ at the bottom to 0 at the top of the gap.¹⁵ Matching to a wave function on the $z > z_0$ side of the terminating plane of the form

$$\psi = e^{-ikz} + r_C e^{i\phi_C} e^{+ikz}, \quad (14)$$

we obtain $r_C = 1$ and

$$\kappa \tan(\phi_C/2) = p \tan(pz_0 + \delta) - q. \quad (15)$$

We now have the explicit E dependences of ϕ_B and ϕ_C , and we can solve Eq. (1) for the energies of the surface states. Two principal input parameters are required: the band-gap parameter V_g and the position E_V of the vacuum level. Results for ϕ are shown in Fig. 2 for the case of the $L_{2'} \rightarrow L_1$ band gap at $\bar{\Gamma}(k_x, k_y = 0)$ on Cu(111).

The $n=0$ solution occurs at -0.3 eV relative to the Fermi level E_F , a result in good agreement with a surface state observed at -0.39 eV in angle-resolved photoemission experiments.^{16,17} The $n=1$ state is predicted to occur at -0.8 eV relative to E_V , in reasonable agreement with *k*-resolved inverse-photoemission data.⁶ For $n \geq 2$, ϕ_C has the constant value of π , so that the energies fall on a Rydberg series with $a=0$.

B. Step-potential comparison

It is instructive to establish the connection between the results for an image potential and those for the more standard step potential. Using Eqs. (4) and (15), it is easy to show that the $n=0$ condition ($\phi_C = -\phi_B$) is identical to Eq. (23) of Goodwin's paper¹⁰ and leads to all the standard results of that paper. In particular, the gap must be Shockley-inverted ($V_g > 0$) in order for a surface state to exist.¹⁵

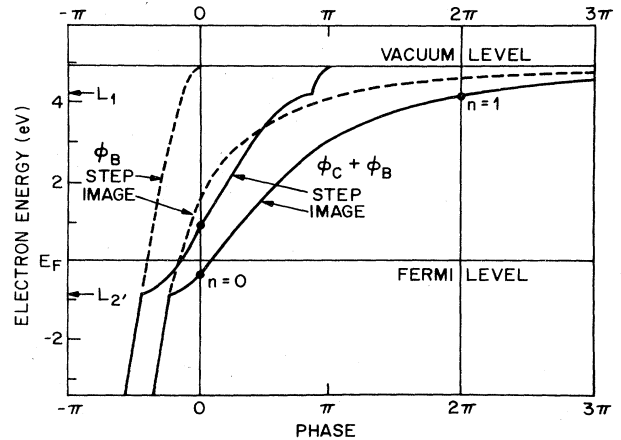


FIG. 2. Energy variation of the reflection phase changes ϕ_B and $\phi_B + \phi_C$ for the L gap in Cu(111).

Numerical values for ϕ_B and ϕ for a step barrier are compared in Fig. 2 with those for the image barrier. This figure illustrates the two basic effects of inclusion of an image-potential barrier: the energy of the existing state is lowered,¹⁸ and additional states are introduced.¹⁹ The $n=0$ solution is the *only* solution in this step-barrier case, and this serves to sharpen the distinction between crystal-induced and image-potential-induced surface states. We may define the $n=0$ solution as the crystal-induced state since it is the state which persists even in the absence of the image-potential asymptotic form for the surface barrier. The expressions "Shockley state," "crystal-induced state," and " $n=0$ state" may be used interchangeably.

The original paper of Johnson and Smith¹ employed a hydrogenic numbering scheme in which the Shockley state (actually a resonance) was designated as the $n=1$ state. The choice between the two numbering schemes is largely a matter of personal taste, provided that all states in the gap and the number of wave-function nodes beyond the image plane are satisfactorily accounted for. The virtues of the present scheme are (1) it recognizes that the condition $n=0$ reproduces standard NFE theory of surfaces states at a step barrier, and (2) the $n=1$ and higher image states are compressed into a narrower energy range so that it is more reasonable to treat ϕ_C , and hence the quantum defect, a , of the Rydberg series as a constant.

C. Zone-boundary case

It is frequently found that a band gap associated with a reciprocal-lattice vector \mathbf{g} can support surface states on surfaces whose normal is not necessarily parallel to \mathbf{g} . The procedure is still to set $k_z = p + iq$ and to solve Eq. (8) for p and q .²⁰ The algebra is more cumbersome, but we do retrieve Eqs. (9)–(12) at the points of high symmetry at the edge of the surface Brillouin zone where $k_x = g_x/2$ and $k_y = g_y/2$.

In expressing the wave function in the region $z < z_0$, it is conventional to invoke the symmetry operation $k_{||} \rightarrow -k_{||}$ and to form the even and odd combinations^{20,21}

$$\psi^+ = e^{qz} \cos(k_{||} r_{||}) \cos(pz + \delta), \quad (16)$$

$$\psi^- = e^{qz} \sin(k_{||} r_{||}) \sin(pz + \delta). \quad (17)$$

The corresponding expressions for the phase change on reflection at the crystal are

$$\kappa \tan(\phi_C^+/2) = p \tan(pz_0 + \delta) - q, \quad (18)$$

$$\kappa \tan(\phi_C^-/2) = -p \cot(pz_0 + \delta) - q. \quad (19)$$

There are thus two branches of the ϕ_C curve, and we have the possibility of *two* $n=0$ surface states in the same gap.^{20,21} Since we place the origin on a surface atom, the wave function ψ^+ is s -like within the surface layer ($s_{||}$ -like) in the sense that it places its amplitude on the surface atoms, whereas ψ^- is $p_{||}$ -like in that its amplitude lies between surface atoms. Perpendicular to the surface layer, ψ^+ (ψ^-) is p_{\perp} -like (s_{\perp} -like) at the bottom and s_{\perp} -like (p_{\perp} -like) at the top of the gap.

Surface states derived from the two branches will differ in energy because of the *surface-corrugation* potential. In

the present model, the parameter V_g plays two roles. Firstly, it brings about, at the boundaries of the *bulk* Brillouin zone, the energy gaps which can support surface states. Secondly, since \mathbf{g} has a component parallel to the surface, there is a contribution $2V_g \cos(k_{||} r_{||})$ to the surface-corrugation potential which creates a gap at the boundary of the surface Brillouin zone between the wave functions of $s_{||}$ and $p_{||}$ symmetry. In cases where two such surface states are actually observed—and these cases do occur in practice—their energy separation is a measure of the surface-corrugation potential.

D. Alternative crystal termination

Instead of terminating the crystal at $z=z_0$, an alternative procedure would be to terminate at $z=0$ and then allow the electrons to propagate freely in the range $0 < z < z_0$. The crystal phase changes associated with reflection at $z=z_0$ are now rewritten:²²

$$\phi_C^+ = \phi_{C0}^+ + 2\kappa z_0, \quad (20)$$

$$\kappa \tan(\phi_C^+/2) = p \tan \delta - q, \quad (21)$$

$$\kappa \tan(\phi_C^-/2) = -p \cot \delta - q. \quad (22)$$

Since both terminations are artificial, there is no compelling reason to prefer one over the other. Both methods have been used here in the calculation of ϕ_C^{\pm} . Comparison between the results provides some estimate of the quantitative credibility of the phases. Differences arise through the distinction between κ and p on traversing the gap. Since we shall be taking z_0 at half an interlayer spacing beyond the outermost atomic layer, we shall refer to the previous termination as the "half-layer termination." We shall refer to this alternative termination as the "in-layer termination."

IV. APPLICATIONS AND DISCUSSION

A. The L gap in copper

The $L_2' \rightarrow L_1$ band gap in bulk Cu is Shockley-inverted and is associated with \mathbf{g} vectors of the (1,1,1) type. It occurs at $\bar{\Gamma}$ on Cu(111), at \bar{Y} on Cu(110), and at \bar{X} on Cu(001). An ample amount of experimental data is available on both occupied and unoccupied surface states on these surfaces, thus providing an opportunity to test the systematics of the phase-analysis model. A reasonable simulation of the experimental band structure²³ along the $\Gamma(\Lambda)L$ direction is obtained with $V_g = 2.55$ eV and with the Fermi level at 0.85 eV above L_2' . The other needed parameters are $E_g (= 10.3$ eV) (Ref. 24) and the work functions of Cu(111), Cu(110), and Cu(001), which are 4.94, 4.48, and 4.59 eV, respectively.²⁵ Taking z_0 at half an interlayer spacing beyond the outermost atomic layer, we have $p z_0 = \pi/2$ for $\bar{\Gamma}$:Cu(111) and $p z_0 = \pi/4$ for both \bar{Y} :Cu(110) and \bar{X} :Cu(001).

The behavior of ϕ_C^+ and ϕ_C^- and a graphical solution for the energies of the $n=0$ surface states in the various L gaps are shown in Fig. 3. Solutions are shown for both image and step barriers and for both the half-layer and in-layer terminations. Horizontal arrows marked "X" in

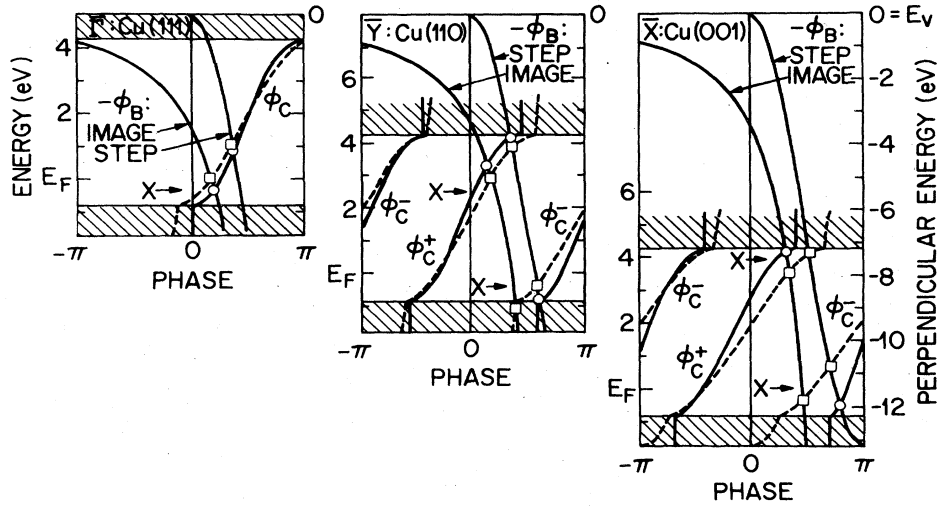


FIG. 3. Graphical solutions (indicated by open circles and squares) for the energies of the $n=0$ surface states associated with the L gap on Cu(111), Cu(110), and Cu(001). Solutions are shown using both the pure image and step forms for $-\phi_B$ and for values of ϕ_C^\pm derived from both the half-layer termination (solid curves) and in-layer termination (dashed curves) of the crystal wave functions. Horizontal arrows marked "X" indicate the experimentally determined energies.

Fig. 3 indicate the experimental surface-state energies measured in photoemission^{16,17,26,27} and inverse-photoemission^{21,28} experiments. There is reasonable accord between theory and experiment for both the existence and approximate energies of surface states.

The \bar{Y} :Cu(110) and \bar{X} :Cu(001) gaps contain two $n=0$ states. As noted above, the energy separation between these states provides an estimate of the amplitude of the surface-corrugation potential. See Sec. IVE for further discussion.

B. The X -gap in copper

The $X_4 \rightarrow X_1$ band gap in bulk Cu is Shockley-inverted and is associated with \mathbf{g} vectors of the (0,0,2) type. It occurs at $\bar{\Gamma}$ on Cu(001) and at \bar{X} on Cu(110). The X gap is larger and lies higher in energy than the L gap. A reasonable simulation of the experimental band structure²³ along the $\Gamma(\Delta)X$ direction is obtained with $V_g = 3.05$ eV, $E_g = 13.45$ eV,²⁴ and with E_F at 1.8 eV below X_4 . We have $pz_0 = \pi/2$ for $\bar{\Gamma}$:Cu(001) and $pz_0 = \pi/4$ for \bar{X} :Cu(110).

Experimental^{29,30} and theoretical energies for the $n=0$ surface states associated with the X gap are compared in Fig. 4. Conclusions are essentially the same as for the L gap. One minor difference concerns the crystal-induced state at $\bar{\Gamma}$:Cu(001). Since E_V lies at midgap, the $n=0$ solution occurs below X_4 , implying a surface resonance rather than a surface state.^{6,30} The different relative position of E_V also implies, through the different values of ϕ_C , that the $n=1$ image state will have a lower binding energy at $\bar{\Gamma}$:Cu(001) than at $\bar{\Gamma}$:Cu(111). This is in agreement with available inverse-photoemission data.^{3,6}

The predicted energies of surface states ($n=0$ and $n=1$) X and L gaps of Cu are summarized in Table I,

where they are compared with the experimental values and the values obtained in various slab calculations.³¹⁻³⁴

C. Empirical barrier phase

A common assumption is that the surface barrier is one dimensional in that it is a function only of z , implying that ϕ_B is a function only of the perpendicular energy ϵ . This can be tested to some extent by taking the experimental energies of the surface states in Table I and plotting the presumptive values of $(\epsilon - E_V)$ versus the presumptive values of $2\pi n - \phi_C^\pm$. One thereby generates the "experimental" data for ϕ_B shown in Fig. 5.

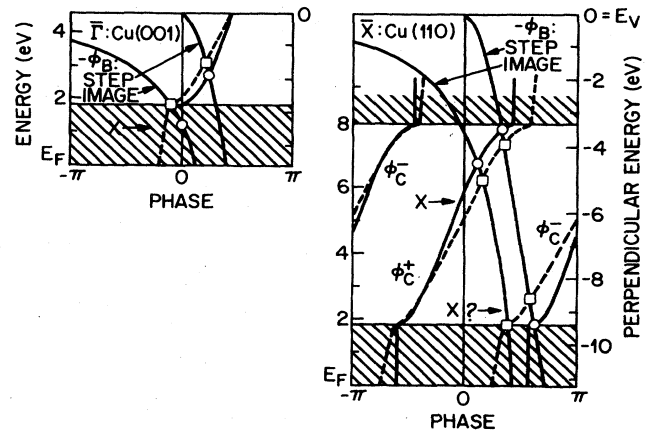


FIG. 4. Graphical solutions for the $n=0$ surface states and/or resonances associated with the X gap on Cu(001) and Cu(110). Terminology is the same as in Fig. 3.

TABLE I. Energies (in eV) of surface states associated with the L and X gaps in copper. Energies are expressed relative to the Fermi level for crystal-induced ($n=0$) states and to the vacuum level for image-potential-induced ($n=1$) states. Predictions are listed for both pure image and step barriers and for both of the alternative crystal terminations discussed in the text.

	Gap type	Half-layer termination		In-layer termination		Expt.	Ref.	Slab calc.	Ref.	
		Image	Step	Image	Step					
$n=0$ (relative to E_F)										
$\bar{\Gamma}$:Cu(111)	L	-0.3	+1.0	-0.0	+0.8	-0.39	17	-0.58	33	
\bar{Y} :Cu(110)	$p_{ }$		-0.8	-1.2	-0.4	-0.39	26	-0.24	31	
	$s_{ }$	L	+3.2	+4.1	+2.9	+3.8	+2.5	21	+1.85	31
\bar{X} :Cu(001)	$p_{ }$	L		-0.6	-0.4	+0.6	-0.06	27	-0.07	32
	$s_{ }$	L	+4.2		+3.5	+4.1	+3.9 ^a	28	+3.4	32
$\bar{\Gamma}$:Cu(001)	X	+1.2	+2.7	+1.8	+3.0	+1.15	30	+0.5	34	
\bar{X} :Cu(110)	$p_{ }$	X		+1.8	+1.8	+2.5	+2.2 ^b	29	2.2	31
	$s_{ }$	X	+6.7	+7.8	+6.2	+7.3	+5.5	29		
$n=1$ (relative to E_V)										
$\bar{\Gamma}$:Cu(111)	L	-0.8		-0.8		-0.9	6			
$\bar{\Gamma}$:Cu(001)	X	-0.5		-0.5		-0.64	3	-0.6	34	

^aExtrapolated.

^bTentative.

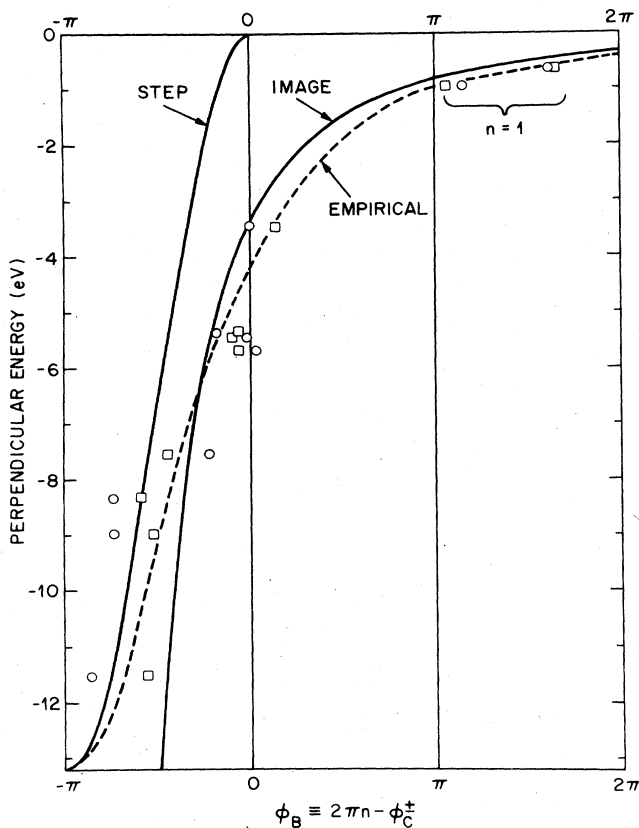


FIG. 5. "Experimental" data for the variation of the barrier phase change ϕ_B with energy. Using the experimentally determined surface-state energies, the presumptive values of the perpendicular energy (actually $\epsilon - E_V$) have been plotted against the presumptive values of $2\pi n - \phi_C^\pm$. Open circles and squares correspond to ϕ_C^\pm values obtained from the half-layer and in-layer terminations, respectively.

McRae and Kane¹⁴ have computed the variation of ϕ_B with ϵ for various saturations of the image barrier. The dashed curve of Fig. 5 has been hand drawn in a way qualitatively consistent with their conclusions, being step-like in the lower part of the inner-potential well, crossing the pure image curve for ϕ_B somewhere near the middle of the well, and becoming imagelike on approaching the vacuum level. The values of ϕ_C^\pm derived from the in-layer termination (squares in Fig. 5) lend themselves better to obtaining a smooth curve for ϕ_B .

D. Effective masses

In the vicinity of the high-symmetry points discussed so far, the surface-state energies disperse as a function of $k_{||}$, leading to measurements of the effective mass m^* . Predictions for the dispersions of the $n=0$ and $n=1$ states using the present model (with half-layer termination) are shown for Cu(111) in Fig. 6.

On moving away from $\bar{\Gamma}$, the width of the projected gap shrinks, requiring a decreasing value of V_g . As a consequence, the lower edge of the gap disperses more rapidly than free-electron-like, whereas the upper edge is relatively flat. These characteristics are shared respectively by the $n=0$ and $n=1$ states which lie close to these edges.

A model based on a single pseudopotential parameter appears to be inadequate for the description of further details. For example, the $n=0$ state in Fig. 6 is predicted to lie always within the gap, whereas the experimental inverse-photoemission data⁶ indicate that the state crosses into the bulk continuum, becoming a surface resonance. We may conclude qualitatively that $m^* > m$ ($m^* < m$) in the upper (lower) part of such a gap, with the inequalities becoming progressively stronger on approaching the band edges.

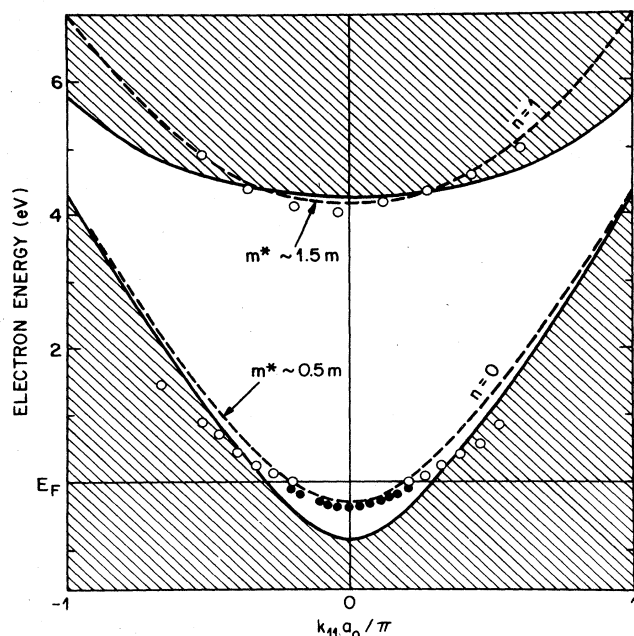


FIG. 6. Dispersion with $k_{||}$ of the $n=1$ image state and the $n=0$ Shockley state near $\bar{\Gamma}$ on Cu(111). The cross-hatched area is the projection of the bulk band structure. The dashed curves are the predictions of the phase-analysis model. The solid and open circles represent, respectively, the photoemission and inverse-photoemission data of Refs. 17 and 6.

E. Surface corrugation

It has been proposed that the effective masses of the image states are enhanced by surface corrugation.³⁵ Such effects should be rather small, however, since the wave functions for $n \geq 1$ are well removed from the surface atomic layer so that they feel a much smoothed surface corrugation.^{34,36}

The wave function of the $n=0$ state, on the other hand, can place its amplitude on the outermost atomic layer, and therefore feel the full surface corrugation. As stated in Sec. III C, when two surface states (one $p_{||}$ -like and one $s_{||}$ -like) are observed in the same gap at the boundary of the surface Brillouin zone, their energy separation is a measure of the surface-corrugation potential. Inspection of Figs. 3 and 4 shows that the measured energy separations in the \bar{Y} :Cu(110) and \bar{X} :Cu(110) gaps tend to be smaller (by $\sim 30\%$) than those predicted by the simple NFE approach. This suggests that in the outermost surface layer some smoothing of the surface-corrugation potential can already be detected.

F. Work-function variation

One of the principal parameters of the model is the position of the vacuum level E_V . Angle-resolved photoemission measurements show that the position of the surface state at $\bar{\Gamma}$:Cu(111) moves to lower energy as the work function is lowered by the adsorption of alkali metals.³⁷ The energy shift, however, is only $\sim 20\%$ of the work-function change. This is just what one expects from the present model if one assumes that the only effect of adsorption is to change the work function.³⁸ In the energy range near the bottom of the L gap, ϕ_C varies much more slowly with E than does ϕ_B . A large change in E_V therefore brings about a relatively small change in the $\phi_C + \phi_B = 0$ energy position.

V. CLOSING REMARKS

The degree of quantitative agreement seen above is surprisingly good for such a simple model. Part of it is presumably due to a fortunate choice for the free parameter z_0 . It is well established that surface-state energies and the work function are correctly reproduced only in calculations which have been performed self-consistently. The real value of the present model lies in the insight it offers into the systematics of surface-state formation and in the scheme it offers for the codification of such states.

The model can be made reliable quantitatively from an empirical point of view. Specifically, the empirical form for ϕ_B (dashed curve in Fig. 5) combined with the *in-layer* termination values for ϕ_C^\pm reproduces the energies of all ten surface states considered here with a rms accuracy of 0.2–0.3 eV and a maximum deviation of 0.5 eV. The model could therefore be quite useful in predicting the probable energy locations of surface states or resonances in cases where first-principles self-consistent calculations are not available.

The perpendicular energies of the ten surface states and/or resonances discussed here span the entire range of the inner-potential well. The need to reproduce the energies of these states should impose severe constraints on any acceptable form for the surface barrier, especially in the interesting changeover region between steplike and imogelike behavior.

ACKNOWLEDGMENTS

It is a pleasure to acknowledge conversations with E. G. McRae, upon whose methods the phase analysis of this paper is based. I have benefited also from discussions with S. L. Hulbert, P. D. Johnson, S. D. Kevan, and M. Weinert, and from early communications of the work of R. A. Bartynski and T. Gustafsson.

¹P. D. Johnson and N. V. Smith, Phys. Rev. B 27, 2527 (1983).

²V. Dose, W. Altmann, A. Goldmann, U. Kolac, and J. Rogozik, Phys. Rev. Lett. 52, 1919 (1984).

³D. Straub and F. J. Himpsel, Phys. Rev. Lett. 52, 1922 (1984).

⁴D. A. Wesner, P. D. Johnson, and N. V. Smith, Phys. Rev. B 30, 503 (1984).

⁵B. Reihl, K. H. Frank, and R. R. Schlittler, Phys. Rev. B 30, 7328 (1984).

- ⁶S. L. Hulbert, P. D. Johnson, N. G. Stoffel, W. A. Royer, and N. V. Smith, *Phys. Rev. B* **31**, 6815 (1985); N. V. Smith, *Appl. Surf. Sci.* (to be published).
- ⁷E. G. McRae, *Rev. Mod. Phys.* **51**, 541 (1979).
- ⁸E. G. McRae, *Surf. Sci.* **25**, 491 (1971).
- ⁹P. M. Echenique and J. B. Pendry, *J. Phys. C* **11**, 2065 (1978).
- ¹⁰E. T. Goodwin, *Proc. Cambridge Philos. Soc.* **35**, 205 (1939).
- ¹¹A. W. Maue, *Z. Phys.* **94**, 717 (1935).
- ¹²V. Heine, *Proc. R. Soc. London* **81**, 300 (1962).
- ¹³D. S. Boudreaux and V. Heine, *Surf. Sci.* **8**, 426 (1967).
- ¹⁴E. G. McRae and M. L. Kane, *Surf. Sci.* **108**, 435 (1981).
- ¹⁵The sign convention for V_g depends on the choice of the $z=0$ origin. See F. Forstmann, in *Photoemission and Electronic Properties of Surfaces*, edited by B. Feuerbacher, B. Fitton, and R. F. Willis (Wiley, New York, 1978).
- ¹⁶P. O. Gartland and B. J. Slagsvold, *Phys. Rev. B* **12**, 4047 (1975).
- ¹⁷S. D. Kevan, *Phys. Rev. Lett.* **50**, 526 (1983).
- ¹⁸M. Kolar and I. Bartos, *Czech J. Phys. B* **23**, 179 (1973).
- ¹⁹N. Garcia and J. Solana, *Surf. Sci.* **36**, 262 (1973).
- ²⁰J. E. Inglesfield and B. W. Holland, in *The Chemical Physics of Solid Surfaces and Heterogeneous Catalysis*, edited by D. A. King and D. P. Woodruff (Elsevier, New York, 1981).
- ²¹R. A. Bartynski, T. Gustafsson, and P. Soven, *Phys. Rev. B* **31**, 4745 (1985).
- ²²The free-propagation contribution $2\kappa z_0$ to the round-trip phase accumulation has been lumped into ϕ_C for purposes of convenience in comparisons. It is more customary (see Refs. 8, 9, and 14) to lump the $2\kappa z_0$ term into ϕ_B .
- ²³J. Knapp, F. J. Himpsel, and D. E. Eastman, *Phys. Rev. B* **19**, 4952 (1979).
- ²⁴The value of E_g needs to be larger than its free-electron value in order to offset the deficiency of the simple NFE model that it splits the band edges symmetrically: $E_g \pm |V_g|$. The actual gaps in Cu are asymmetrical about the free-electron E_g due to hybridization and orthogonalization with the Cu d bands. The use of an enhanced E_g is equivalent to the use of a reduced crystalline effective mass.
- ²⁵P. O. Gartland, *Phys. Norv.* **6**, 201 (1972), quoted in *CRC Handbook of Chemistry and Physics*, 65th ed., edited by R. C. Weast (Chemical Rubber Co. Boca Raton, FL, 1984).
- ²⁶S. D. Kevan, *Phys. Rev. B* **28**, 4822 (1983).
- ²⁷S. D. Kevan, *Phys. Rev. B* **28**, 2268 (1983).
- ²⁸V. Dose, U. Kolac, G. Borstel, and G. Thorner, *Phys. Rev. B* **29**, 7030 (1984).
- ²⁹R. A. Bartynski and T. Gustafsson (private communication).
- ³⁰D. P. Woodruff, S. L. Hulbert, P. D. Johnson, and N. V. Smith, *Phys. Rev. B* **31**, 4046 (1985).
- ³¹D. G. Dempsey and L. Kleinman, *Phys. Rev. B* **16**, 5356 (1977).
- ³²A. Euceda, D. M. Bylander, L. Kleinman, and K. Mednick, *Phys. Rev. B* **27**, 659 (1983).
- ³³A. Euceda, D. M. Bylander, and L. Kleinman, *Phys. Rev. B* **28**, 528 (1983).
- ³⁴M. Weinert (private communication).
- ³⁵N. Garcia, B. Reihl, K. H. Frank, and A. R. Williams, *Phys. Rev. Lett.* **54**, 591 (1985).
- ³⁶Equation (3) of Ref. 35 overestimates the enhancement of the effective mass by a factor of 4, an error which renders the detailed arguments of that paper untenable.
- ³⁷S. A. Lindgren and L. Walldén, *Solid State Commun.* **28**, 283 (1978); **34**, 671 (1980).
- ³⁸P. Ahlqvist, *Solid State Commun.* **31**, 1029 (1979).